Linearly Sweeping Leaky-Wave Antenna with High Scanning Rate

Jianfeng Chen, Wei Yuan, Wen Xuan Tang, *Member, IEEE,* Lei Wang, *Senior Member, IEEE,* Qiang Cheng, *Member, IEEE,* and Tie Jun Cui, *Fellow, IEEE*

***Abstract*—Leaky wave antenna is known as a type of travelling antenna with dispersive frequency responses, which has found important applications in modern communication, imaging and radar systems. The beam scanning rate is a key consideration in some applications, since it can minimize the bandwidth requirement of the system, during the scanning in broad angular regions. However, the sweeping linearity, namely the scanning angular range per unit frequency, is seldom taken into account at the same time in the published literature. In this article, we propose a waveguide-type leaky-wave antenna working from 11.1 GHz to 12 GHz. By loading periodical pins with glide symmetry in the waveguide, it is possible to manipulate the dispersion properties of the fast wave mode, hereby giving rise to a good balance between the scanning rate and sweeping linearity. This scenario has been validated by numerical simulation and experiment with excellent agreement. The measurement results reveal that the scanning angles have been increased to range from 16.7° $\sim$67.5° varying the frequency from 11.1 to 12.1 GHz. The relative average scanning rate is enhanced up to 589.3°, with high sweeping linearity.**

***Index Terms*—Glide symmetry, leaky-wave antenna, linearity, scanning rate.**

I. Introduction

LEAKY wave antennas (LWAs) are defined as travelling-wave antennas with the outstanding frequency scanning ability. The electromagnetic waves can be gradually leaked out into free space as they propagate along the guided wave structures, leading to narrow beams in forward or backward directions. Due to the dispersive properties of the leaky mode, the beam direction can be effectively varied with the frequency, enabling the beam scanning within a finite bandwidth [1], [2]. Depending on the ratio between the propagation constant and the free space wavenumber, LWAs can be divided into two groups: fast-wave mode LWAs and slow-wave mode LWAs. To realize a fast-wave mode LWA, we can cut a continuous slot or sub-wavelength slots directly along the waveguide, allowing the wave radiated directly in free space. However, the slow-wave mode LWA are usually constructed by periodically modulated transmission line that can only radiate the energy with space harmonics [3].

Owing to the advantages of low cost, simple geometry and broad bandwidth, LWAs play an important role in some special scenarios. The frequency-dependent beam-scanning characteristic of LWAs permits the conversion from the temporal frequency spectrum into the spatial frequency spectrum [4], e.g. time-space Fourier transform. Such unique property has been exploited to develop real-time spectrum analyzer [5], radar sensors [6]–[8] and holographic images [9]–[11].

So far lots of efforts have been devoted to improving the beam scanning range of LWAs. Traditional uniform or quasi-uniform LWAs can only radiate in the front quadrant [3]. In contrast, periodically modulated LWAs are capable of both forward and backward scanning [12], but usually fail to achieve broadside radiation because of the open stopband (OSB) phenomenon [13]. Such limitation can be addressed by employing asymmetrical elements [14]–[16], which are capable of reducing the width of the OSB and improving impedance matching. A continuous backfire-to-endfire scanning ability without OBS can also be realized with the composite right-/left-handed (CRLH) transmission lines, owing to the continuous dispersion curve and non-zero group velocity in the broadside [17].

The scanning rate of LWAs is an important measure to assess the property of time-space transformation [4]. For an LWA with a low scanning rate, a signal with a wide bandwidth can be radiated into a limited angular range. In addition, in the case of zero scanning rate, LWAs can possess a fixed beam [18], [19], which is important for point-to-point communication and large capacity communication with wide bandwidth. On the contrary, LWAs with high scanning rate can realize wide angle scanning in narrowband. This is especially beneficial for band limited RF transceivers and A/D converters. Intensive interests have been attracted to increase the scanning rate of the LWAs [20]–[23].

Another indicator to describe the quality of time-space transformation is the sweeping linearity of the antennas. Ideally, the radiation beam can sweep across the desired angle range uniformly, under the condition of linear the scanning rate. However, the nonlinearity is inevitable due to the dispersive nature of traditional LWAs (quasi-hyperbolic scanning law [24]), hereby making it hard to accomplish this goal as expected. Aiming to address this challenge, the down converters and signal processors of the radar and communication systems need to be designed deliberately to make corrections for radar applications [5].

Manuscript received November 4, 2020; revised XX XX, XXXX.

This work is supported by the National Key Research and Development Program of China (2017YFA0700201, 2017YFA0700202, 2017YFA0700203), the National Natural Science Foundation of China (61631007, 61571117, 61138001, 61371035, 61722106, 61731010, 11227904), and the 111 Project (111-2-05).*(Corresponding author: Qiang Cheng.)*

J. Chen, W. Yuan, W. X. Tang, Q. Cheng and T. J. Cui are with the State Key Laboratory of Millimeter Waves, Southeast University, Nanjing 210096, China (e-mail: qiangcheng@seu.edu.cn and tjcui@seu.edu.cn).

L. Wang is with School of Engineering and Physical Sciences, Heriot-Watt University, Edinburgh EH14 4AS, U.K (e-mail: wanglei@ieee.org).

This article has been accepted for publication in a future issue of this journal, but has not been fully edited. Content may change prior to final publication. Citation information: DOI 10.1109/TAP.2020.3037830, IEEE Transactions on Antennas and Propagation

In general, it is quite difficult to find a balance between the scanning rate and the sweeping linearity. Since any tiny fluctuation of the dispersion curve for the propagation constant in an LWA will be enlarged in the spatial spectrum, if the scanning rate is very high. To the best of authors' knowledge, there has been no LWAs with linear scanning rate discussed in the previous literature.

In this paper, we propose a fast-wave mode LWA to achieve high scanning rate and good sweeping linearity simultaneously. The antenna is periodically loaded by metallic pins with glide symmetry, which has been introduced in [25]–[31], and employed in several microwave devices including transmission lines [32], [33], phase shifters [34], [35], filters [36] and antennas [18], [19], [21], [37]. Since the antenna dispersion can be effectively manipulated by the artificial elements, it is easy to control the propagation constant of the leaky modes, and therefore adjust the leaky rate of the LWA. Moreover, thanks to the excellent linearity of the dispersion curve for periodic pin structures with glide symmetry, the sweeping linearity can also be significantly improved. The optimized LWA owns a constant relative average scanning rate (RASA, defined by dividing scanning range and average bandwidth) of 589.3 degrees (50.8 degrees, from 11.1 to 12.1 GHz), while keeping good performance on the radiation gain and the sidelobe level in the whole operating band.

The contents of this paper are organized as follows. In Section II, the configuration of our proposed LWA and the principle of high and linear scanning rate are introduced. The operation mechanism of the LWA and the detailed feeding structure are presented in Section III. The simulation and experimental results are provided in Section IV, along with relevant discussions. Finally, the conclusion is given in Section V.

II. Configuration and Principle

A. Configuration

Fig. 1 presents the schematic of the proposed leaky-wave antenna. It is actually a metallic waveguide structure, including two feeding parts and one radiation part. The metallic corrugations on top and bottom surfaces are employed as a high impedance surface to suppress the conducting current, which can decrease the backward radiation of LWA [38]. The double-row leaky pins on the radiating aperture of the LWA, provide an avenue for tailoring the leakage rate by changing the pin dimensions. As illustrated in Fig. 1(b), the inside of the waveguide is also filled with metallic pins with different dimensions and periods, in order to support the TE_{30} mode as the required leaky mode of the proposed LWA.

The cross-section view of the radiation part is sketched in Fig. 2, including the transverse (xoz plane) and longitudinal (yoz plane) cross sections. It can be divided into two sections: the waveguide section and the leakage section. In the former section, three pairs of pins are included in the transverse direction of the waveguide and distributed on the upper and lower surfaces respectively. From Fig. 2(b), it is clear that the upper green pins are of glide symmetry with the lower blue pins in the longitudinal direction, as can efficiently manipulate

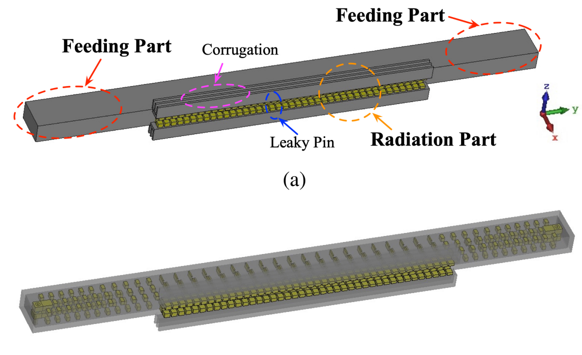

Fig. 1. (a) Illustration of the proposed LWA with high scanning rate and linearity. (b) Perspective view of the LWA.

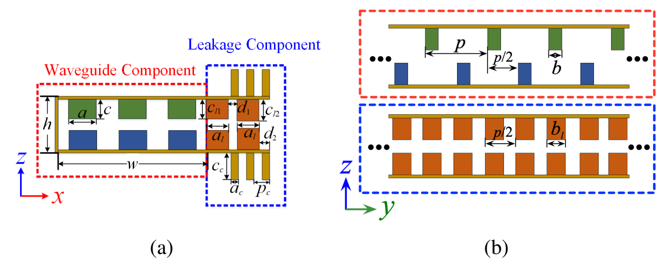

Fig. 2. Cross-section views of the radiation part at the (a) transverse section and (b) longitudinal sections of waveguide and leakage components.

the dispersion property of the propagation mode. In the latter section, there are two rows of metallic pins and corrugations. Note that the pins at the radiation aperture are no longer placed with glide symmetry, since they are only used to tailor the leakage rate of the output beam as depicted in Fig. 2(b).

Fig. 3 shows the cross-section view of the left feeding part in Fig. 1(a). As the right feeding part has identical geometry with the left one, it will not be discussed separately for simplicity. The feeding structure is composed of a mode generator and a taper, as demonstrated in Fig. 3(a). The mode generator is constituted by a coaxial-waveguide converter and periodic pins with normal symmetry in the longitudinal section. The taper part in Fig. 3(a) is used to transform the periodic pins from normal symmetry to glide symmetry for the purpose of impedance matching, where the longitudinal shift between the upper and lower pins is gradually increased from 0 to a half period $p_f/2$. The dimensions of the proposed LWA are listed in Table I.

TABLE I
Dimensions of the Proposed LWA

Parameters	w	h	a	b	c	a_l	b_l
Value (mm)	28.5	13	7	1	4.5	5	5
Parameters	c_{l1}	c_{l2}	a_f	b_f	c_f	a_r	b_{r1}
Value (mm)	5	2.5∼4.3	5	3	3.9	7	7
Parameters	b_{r2}	c_{r1}	c_{r2}	a_c	c_c	d_1	d_2
Value (mm)	9	5.2	3	2	10	1.5	1.5
Parameters	d_3	d_4	p	p_c	p_{f1}	p_{f2}	
Value (mm)	2.5	1.5	13	6.5	9	10.5	

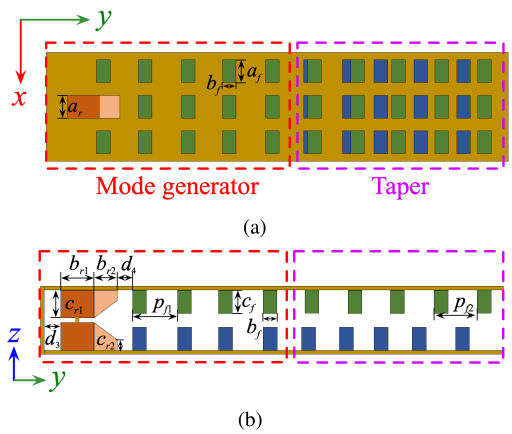

Fig. 3. Cross-section views of the feeding part. (a) xoy plane. (d) yoz plane.

B. Definition of Scanning Rate

The beam direction of leaky-wave antennas can be expressed as:

$$\theta = \arcsin(\frac{\beta}{k_0}). \quad (1)$$

where β is the propagation constant of the leaky mode, and k_0 is the wave number in free space. Due to the frequency dependence of β and k_0, the beam direction θ is also a function of the operation frequency. To describe the scanning rate of the radiation beam in space, we can use the partial derivation of θ with respect to frequency [22]:

$$S(f_0) = \frac{\partial\theta(f_0)}{\partial f} = \frac{1}{k_0 \cos\theta(f_0)}[\frac{\partial\beta}{\partial f} - \frac{2\pi}{c}\sin\theta(f_0)]. \quad (2)$$

From Eq. (2), the scanning speed is closely related to the changing rate of the propagation constant $\partial\beta/\partial f$, as well as the radiation angle at the operation frequency. Obviously, once the radiation angle is determined, a rapid frequency change of β corresponds to a high scanning speed in free space.

In view of the restricted bandwidth of the LWAs, we can further extend the concept of scanning rate defined in Eq. (2) to an average case, which can be expressed as the ratio between the scanning angle range and the antenna bandwidth, as:

$$S_{\text{average}} = \frac{\Delta\theta}{\Delta f} = \frac{\theta_2 - \theta_1}{f_2 - f_1}. \quad (3)$$

Here, θ_1 and θ_2 are the starting and ending angles of the scanning range. f_1 and f_2 correspond to the working frequencies of θ_1 and θ_2. However, it is important to notice that the average scanning rate in Eq. (3) only takes the absolute bandwidth into account. But for normal electronic systems, the relative bandwidth is more important to evaluate their spectrum efficiency. So, it is reasonable to replace the absolute bandwidth Δf in Eq. (3) by the relative bandwidth $\Delta f/f_c$,

$$S_{\text{RASR}} = \frac{\Delta\theta}{\Delta f/f_c}. \quad (4)$$

where S_{RASR} stands for the relative average scanning rate (RASR), and f_c is the central operation frequency.

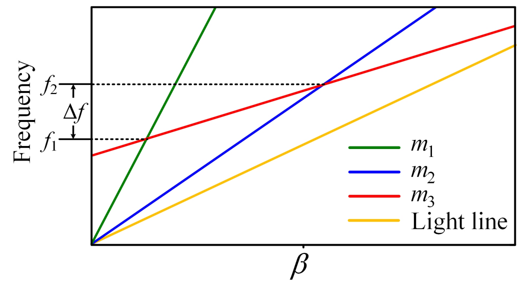

Fig. 4. Schematic of the dispersion curves with fixed radiation angles (green and blue), the assumed link line (red) and the light line (yellow).

C. Principle of High Relative Average Scanning Rate (RASR)

From Eq. (4), it can be seen that we only need to care about the starting and ending radiation angle, namely θ_1 to θ_2, regardless of the beam orientation during the intermediate scanning process. Thus, in the dispersion diagram in Fig. 4, we can easily find two sets of coordinates (f_1, β_1) and (f_2, β_2), corresponding to the starting and ending scanning states of the LWA. Two lines can be drawn from the origin to the two points marked in green and blue, which can be expressed by

$$f = m_1\beta, \text{ starting state.} \quad (5)$$

$$f = m_2\beta, \text{ ending state.} \quad (6)$$

where $m_1 = c/(2\pi\sin\theta_1)$ and $m_2 = c/(2\pi\sin\theta_2)$ respectively.

As mentioned before, the intermediate scanning states can be neglected in the calculation of RASR. Actually, there are many solutions of the antenna dispersion curve passing through the two points. But the simplest choice is the link line between them, as indicated by the red line in Fig. 4, and it can be written as

$$f = m_3\beta + n. \quad (7)$$

From this model, the denominator of Eq. (4) becomes:

$$\frac{\Delta f}{f_c} = \frac{2m_3(m_1 - m_2)}{2m_1m_2 - m_3(m_1 + m_2)}. \quad (8)$$

The general expression of RASR can be rewritten as, as:

$$S_{\text{RASR}} = \Delta\theta[\frac{m_1m_2}{m_3(m_1 - m_2)} - \frac{m_1 + m_2}{2(m_1 - m_2)}]. \quad (9)$$

It can be seen that,the RASR is the monotonic descending function of m_3, when m_1 and m_2 keep constant. It is entirely independent of the central operating frequency, which agrees well with the definition of RASR in Eq. (4). A high RASR can be obtained by reducing the slope m_3.

This article has been accepted for publication in a future issue of this journal, but has not been fully edited. Content may change prior to final publication. Citation information: DOI 10.1109/TAP.2020.3037830, IEEE Transactions on Antennas and Propagation

D. Definition of Scanning Linearity

Different from RASR, the scanning linearity is to describe the fluctuation of the scanning rate within the desired bandwidth. A large linearity reflects a stable speed of beam scanning, which is beneficial to reduce the complexity of post-processing for an LWA based system. This fluctuation can be measured by observing the second partial derivation of the radiation angle θ:

$$L = |\frac{\partial^2 \theta}{\partial f^2}| = |\frac{\partial(\text{Scanning Rate})}{\partial f}|. \tag{10}$$

If an LWA has constant scanning rate, we have zero L, corresponding to a uniformly scanning radiation beam. Obviously, a stable scanning rate is essential to maintain the sweeping linearity.

In our design, the initial frequency n in Eq. (7) is chosen to be 7.5×10^9 Hz. The dispersion curves for different m are demonstrated in Fig. 5(a). The corresponding beam directions and scanning rates are given in Fig. 5(b) based on Eqs. 1-2. A large slope m is unfavorable for increasing the scanning rate but helps to achieve better scanning linearity L in the observation band. So, a proper m is also very important to seek the balance between the scanning rate and scanning linearity.

E. Realization of quasi-linear dispersion relations

In [39], a linear dispersion curve is realized around Γ-point of the Brillouin zone, since the existence of the Dirac cone allows to design a linear LWA with broadside beam in a narrow bandwidth Recent studies suggest that the periodic pins loaded in the waveguide offer an effective mean of dispersion control, which have been widely used to design lens antennas [18], [37]. On this basis, we attempt to introduce periodic loadings into the leaky wave antenna to construct the linear dispersion relation in Eq. 7 and improve the RASR of the antenna.

First, we investigate the dispersion property of the unit cell with normal symmetry, with the simulation setup given in Fig. 6. The full wave package (CST Microwave studio 2016) is employed for numerical simulations. Note that, the periodic boundaries are applied in y-direction, while the PEC boundaries are applied in x and z directions. The metallic pins inside the cell are of the mirror symmetry. The dispersion curves of the proposed unit cell are calculated by the Eigenmode Solver of CST in Fig. 7.

Due to the periodicity of Brillouin zones, only the dispersion curves in the first Brillouin zone ($\beta p = 0 \sim \pi/2$) are provided in this paper. In Fig. 7(a), we can find that the cut-off frequency and the slope of β tend to decrease as the pin height c goes up, which is helpful to improve RASR. The pin width b only affects the working bandwidth as illustrated in Fig. 7(b). Adjusting the width w and period p of the unit cell also lead to the reduction of the slope of β in Fig. 7(c)-(d) and result in an approximately linear dispersion curve as expected. Specifically, a small w can help to reduce the slope effectively and raise the central frequency at the same time. A large period p also gives rise to small slope but contribute less to the shift of the center frequency, as shown in Fig. 7(d). However, it is important to emphasize that, with the increase of the unit period p, the dispersion curve may not intersect with the light line, implying that the maximum radiation angle is less than 90°. The scanning range will be narrowed at the same time. Therefore, a suitable unit period p should be chosen to find satisfactory RASR and scanning range simultaneously.

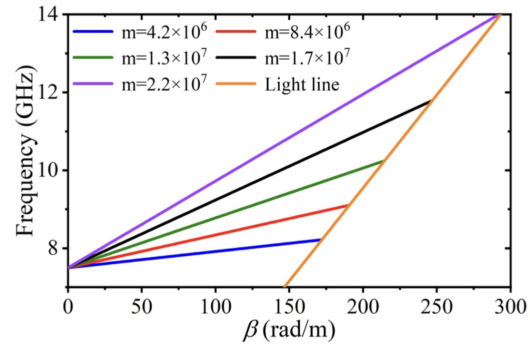

(a)

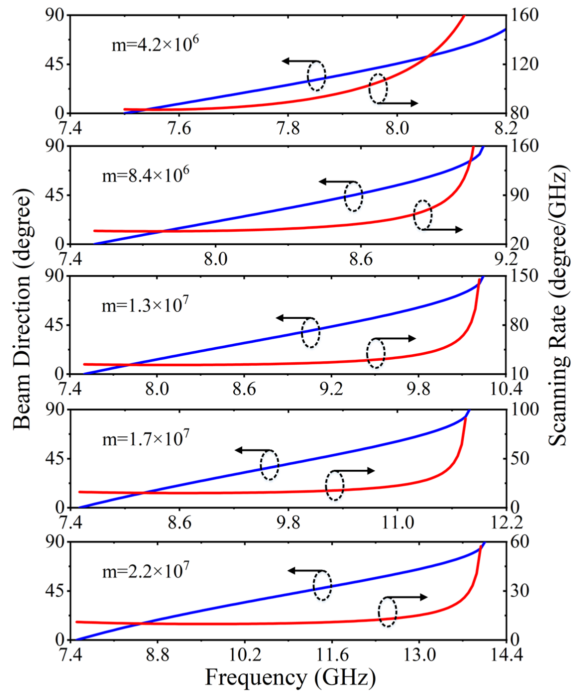

(b)

Fig. 5. (a) Dispersion curves with different m. (b) Beam directions and scanning rates with different m.

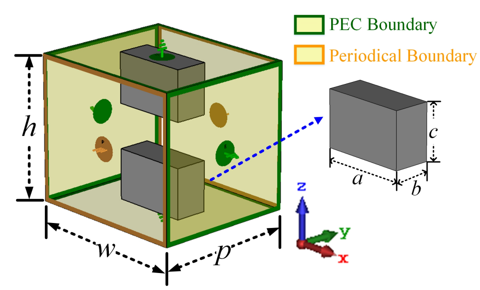

Fig. 6. Simulation configuration of the unit cell, with periodic boundary in the y-direction (two faces with yellow frame) and PEC boundary in the other directions (faces with green frame).

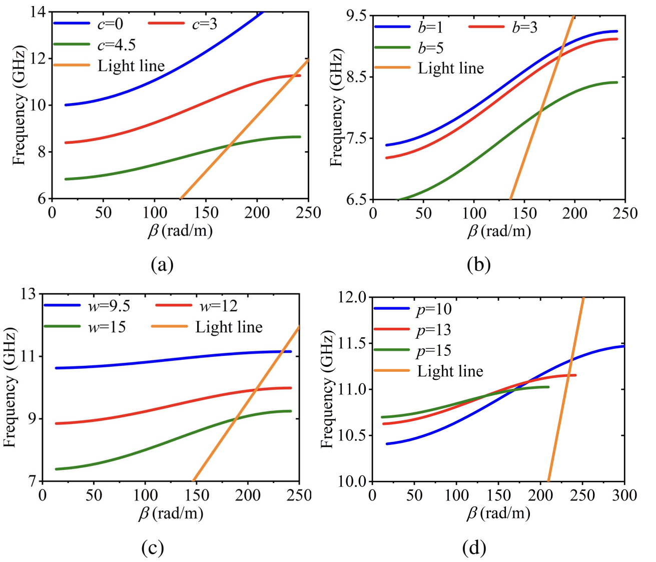

Fig. 7. Dispersion curves of the unit cell as a function of different geometric parameters.

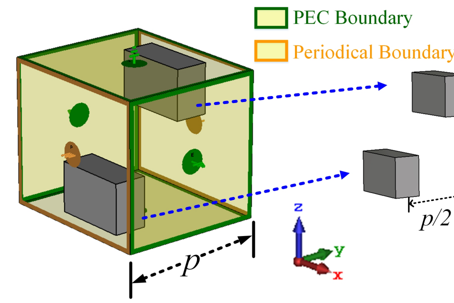

Fig. 8. Simulation configuration of the unit cell with glide symmetry.

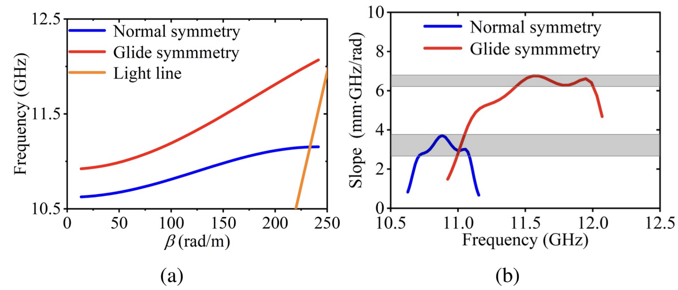

Fig. 9. (a) Dispersion curves and (b) their slopes of the unit cell with normal and glide symmetries.

Targeting for further increasing the linearity of the dispersion curve, a possible recipe is to align the upper and lower pins with glide symmetry [37], [40]. As shown in Fig. 8, the two pins are shifted by a half period along y direction. In this case, the first bandgap is closed, and the dispersion curve is more linear especially near the edge of the bandgap, which is favored by the desired LWA.

To confirm this phenomenon, the dispersion curves and the corresponding slopes for unit cells with normal symmetry and glide symmetry ($w = 9.5$ mm, $h = 13$ mm, $a = 7$ mm, $b = 1$ mm, $c = 4.5$ mm and $p = 13$ mm) are presented in Fig. 9. The linearity of the two curves are good on the whole (see Fig. 9(a)), but the slope fluctuation seems to be smaller for the glide symmetric structure in the operation band in Fig. 9(b). Whereas, the dispersion of the normal symmetric cell possesses a larger slope, which is helpful for improving the RASR. The beam directions and scanning rates of the normal/glide symmetric cells are calculated using Eq. (1) and (2), as shown in Fig. 10. The scanning rate of the glide symmetric cell can be approximately regarded as a constant in the entire band (11.1 $\sim$ 11.9 GHz), which indicates a linear beam scanning from 20° to 60°. The RASR of the proposed unit cell can reach up to 575°.

Since the high RASR and high linearity are a pair of contradictions in the realization from the discussions herein above, we need to find a trade-off between high RASR and linearity when optimizing the parameters of the unit cell.

III. Design and Analysis of the Proposed LWA

A. Operation Principle of LWA

A key problem of the LWA design is how to control the dispersion characteristics and the leakage of the periodically loaded waveguide simultaneously without effecting the propagation constant, since the distortion of the propagation constant will result in performance degradation for the LWA. For a general groove waveguide LWA, periodic leaky pins can be employed at the aperture to radiation the energy and control the leaky rate [38]. Here, we place the periodic leaky pins before several glide symmetric pins to tune the dispersion characteristic as shown in Fig. 11(a), the structural dispersion curve is shown in blue in Fig. 11(d), and the black ideal line corresponds to the glide symmetric unit without leaky pins as depicted in Fig. 8. Note that, the bandwidth is slightly narrowed at the presence of the leaky pins compared to Fig. 9(a). This can be attributed to the increased effective width of the waveguide, since the limited binding ability of the leaky pins compared with PEC wall. In addition, the leaky pins also lead to slight degradation of the curve linearity in Fig. 8(a), due to the fact that the glide symmetry of the unit cell is broken at this time, resulting in the generation of bandgap in $\beta p = \pi/2$ point.

To circumvent this problem, a modified unit cell that can supports high-order TE mode is proposed to reduce the impact of the leaky pins, as shown in Figs. 11(b)-(c). From the classical electromagnetic theory [41], for a rectangular waveguide

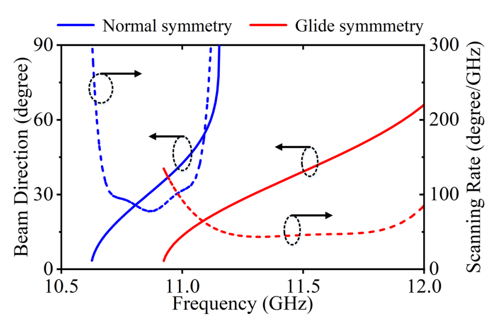

Fig. 10. Beam direction and scanning rate of the unit cell with normal and glide symmetries.

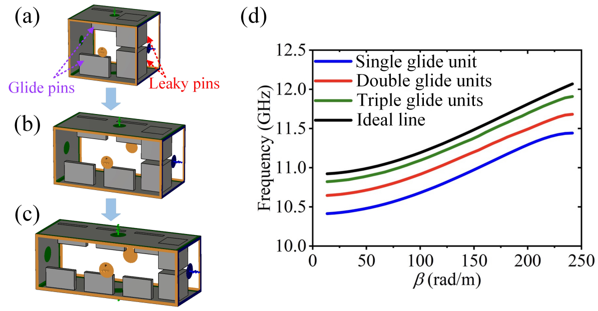

Fig. 11. Candidates of the radiation part. (a)-(c) Unit cells working in the TE_{10}, TE_{20}, TE_{30} mode. (d) Dispersion curves of different unit cells.

with the transverse width nw, the propagation constant of TE_{n0} mode is identical to that of TE_{10} mode in the waveguide with the width of w. It means that we can achieve similar dispersion characteristics if wider waveguide with more glide symmetric elements is employed. Here we consider three waveguides of unequal width, where the operation modes are TE_{10}, TE_{20} and TE_{30} modes respectively (see Figs. 11(a-c)), and the dispersion curves are plotted in Fig. 11(d) for comparison. With the increase of n, the dispersion curve tends to approach the ideal line. In this paper, the waveguide with the width of $3w$ shown in Fig. 3 is used to realize the desired LWA.

Another major concern is the control of leaky rate for the proposed LWA. Also, the propagation constant should not be greatly influenced when tuning the leaky rate. As revealed in [38], [41], the leaky rate is closely related to the dimensions of the leaky pins. By adjusting the pin geometry, the leaky rate of LWA can be controlled freely, which is helpful for reducing sidelobe level and increasing the realized gain [42], [43]. However, the dispersion property is altered at the same time, when different pin heights c_{l1} are considered. Although the differences among the dispersion curves are not significant in Fig. 12(c), it is still not favored for an LWA with high scan rate. To alleviate the effect of the pin height on the dispersion property, double leaky pins are employed at the aperture, which also provides new degree of freedom to control the leaky rate, as shown in Fig. 12(b). Here the height c_{l1} of the inner pins (see Fig. 2(a)) is kept invariant. The dispersion curves for different heights c_{l2} of the outer leaky pins are illustrated in Fig. 12(d). It seems that the double leaky pin structure is a good choice to maintain the stability of structural dispersion.

B. Design of Feeding Part

As discussed above, we use a waveguide that supports TE_{30} mode as the guiding wave part of the LWA. But how to generate this mode with high purity remains to be a challenge. In the past few years, considerable efforts have been devoted to designing the dominant to high-order mode converters. For example, when periodic pins are loaded within the waveguide as illustrated in Fig. 13(a), a certain high-order mode can be generated in desired frequency range, which also forms a bandgap for the rest of modes [43]. Three pairs of pins are

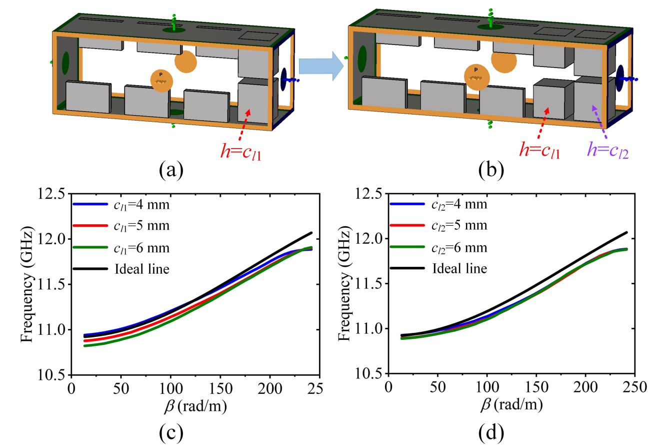

Fig. 12. (a)-(b) Evolution of the proposed unit cell from single leaky pins to double leaky pins. (c) Dispersion curves of the unit cell with different pin height c_{l1} of single leaky pins and (d) with different c_{l2} of double leaky pins and fixed $c_{l1} = 5$ mm.

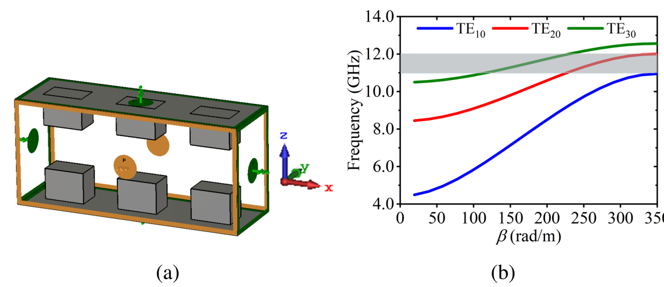

Fig. 13. (a) Unit cell and (b) dispersion curves of proposed TE_{30} mode waveguide.

placed in the transverse direction of the waveguide, with the simulated mode distributions plotted in Fig. 13(b). Note that the upper and lower pins are of mirror symmetry. It can be seen that there exist two waveguide modes from 11∼12 GHz (TE_{20} and TE_{30}, gray region). As discussed in [44], the TE_{20} mode can be suppressed with the central feeding, according to the difference of modal field distributions. Only TE_{30} mode can survive in this waveguide.

The difference between the designs in [44] and this paper is the stimulation of the desired waveguide. The former uses a hollow waveguide to excite the TE_{30} mode. But this is not suitable for our design, since the cut-off frequency (15.8 GHz) of the TE_{30} mode is beyond the operating frequency of our designed LWA. The dimensions of the TE_{30} mode waveguide are listed in Table I. On the contrary, the TE_{30} wave can be excited by a coaxial feeding in the periodically loaded waveguide, due to the increased effective index of the periodic loadings from Fig. 14. Fig. 14 also present the snapshots of electric fields along the waveguide at 11 GHz, 11.5 GHz and 12 GHz. Obviously, TE_{30} mode can be excited efficiently in the whole band. The S-parameters of the proposed TE_{30} waveguide is shown in Fig. 15, where S_{21} is above -1 dB from 11∼11.8 GHz and -2 dB from 11.8∼12 GHz.

This article has been accepted for publication in a future issue of this journal, but has not been fully edited. Content may change prior to final publication. Citation information: DOI 10.1109/TAP.2020.3037830, IEEE Transactions on Antennas and Propagation

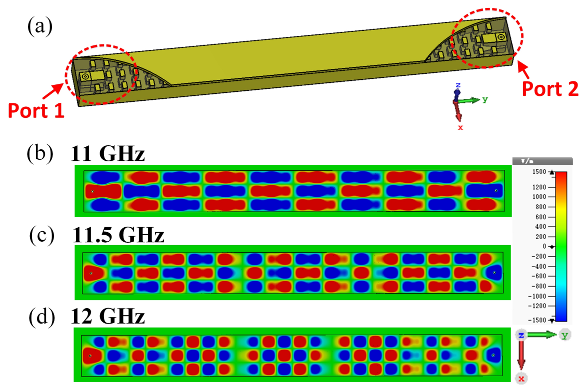

Fig. 14. (a) Schematic of TE_{30} mode waveguide. (b)-(d) Snapshots of the electric field distributions in xoy plane.

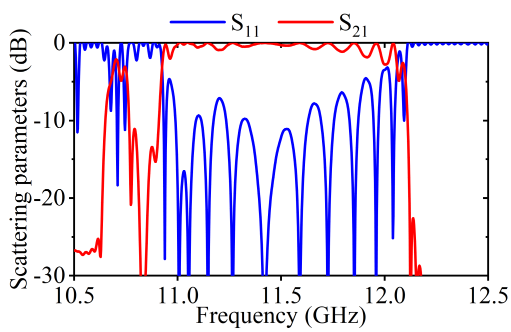

Fig. 15. S-parameters of the proposed TE_{30} mode waveguide.

(a)

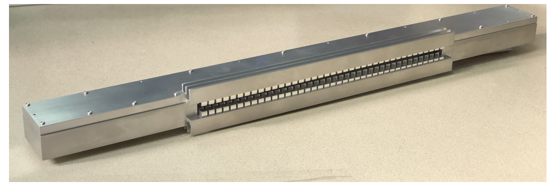

(b)

Fig. 16. Fabricated prototype of the proposed LWA. (a) Internal structure. (b) Overall structure.

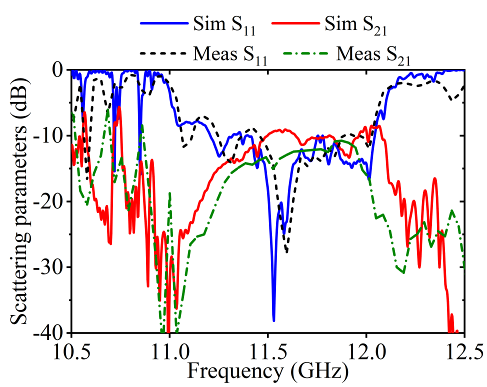

Fig. 17. Simulated and measured scattering parameters for the proposed LWA.

IV. Simulation and Experimental Results

The configurations of our proposed LWA are illustrated in Fig. 1 to Fig. 3 in detail. The radiation part (see Fig. 2) of LWA is designed to support the TE_{30} mode with desired dispersion with high scanning rate and beam linearity, and meanwhile radiate the energy into space efficiently. The corrugations are employed to prevent the production of surface currents which may enhance the backward radiation. Additionally, the feeding part of the proposed LWA (see Fig. 3) is designed to excite TE_{30} mode with high purity. To match the impedances between the feeding part and radiation part, a taper is proposed by converting the pins from normal symmetry to glide symmetry, as shown in Fig. 3.

A prototype of the fabricated LWA is presented in Fig. 16. The simulated and measured results are also compared in this paper. Fig. 17 shows the S-parameters of the LWA. Both $|S_{11}|$ and $|S_{21}|$ are below -10 dB from 11.1 to 12 GHz, implying efficient microwave radiation within this band. A slight red shift of the measured results emerges, mainly due to the fabrication error. The normalized radiation patterns in H-plane are shown in Fig. 18. The sidelobe levels of the LWA are beyond 13 dB from 11.1 to 11.9 GHz. In addition, the radiation angle increases linearly as the frequency grows from Fig. 18. The realized gains ranges from 15.2 to 18 dBi in Fig. 19. The beam direction as a function of the frequency is also given in Fig. 19, showing good scanning linearity as expected. Here the ideal curve (solid red line) is a straight line describing an ideal linear beam scanning, with the average scanning rate 50.8°/GHz, which nearly coincides with the simulated and measured results. The measured linear scanning range is $16.7^\circ \sim 67.5^\circ$ (from 11.1 to 12.1 GHz), and the corresponding RASR is 589.3°. The linearity can be evaluated by calculating the sample standard deviation σ between the simulated/measured angles and ideal radiation angles. Here, the simulated and measured σ values are 0.62° and 1.72°, which indicate an excellent linearity for the radiation beams.

To prove the advantages of our work, we list the results from other reported LWAs in Table. II for comparison. The RASR of those designs are calculated manually from their specifications. The RASR of our design is not the largest compared to other LWAs, since we have to choose a trade-off between high RASR and high linearity, as discussed in Section. II-D. But on the whole, the design antenna exhibits good overall performance. Actually, the RASR can be further improved by simply reducing the symmetry of the unit cell from glide symmetry to normal symmetry, as shown in Fig.10. The linearity comparison is not given in Tab. II due to the lack of data for most published papers.

V. Conclusion

We propose a fast-wave mode leaky-wave antenna with high scanning rate and good sweeping linearity. Periodic pins with normal and glide symmetry are employed in the leaky-wave antenna to manipulate the dispersion of guided modes,

This article has been accepted for publication in a future issue of this journal, but has not been fully edited. Content may change prior to final publication. Citation information: DOI 10.1109/TAP.2020.3037830, IEEE Transactions on Antennas and Propagation

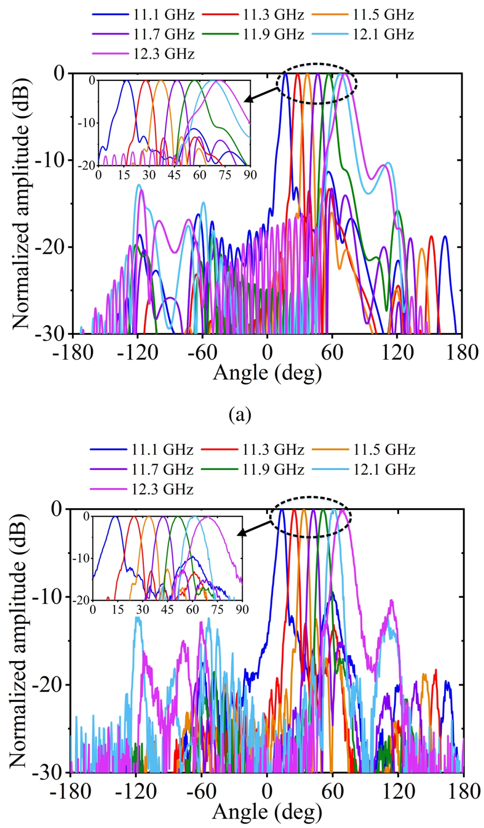

(a)

(b)

Fig. 18. (a) Simulated and (b) measured normalized radiation patterns for the proposed LWA.

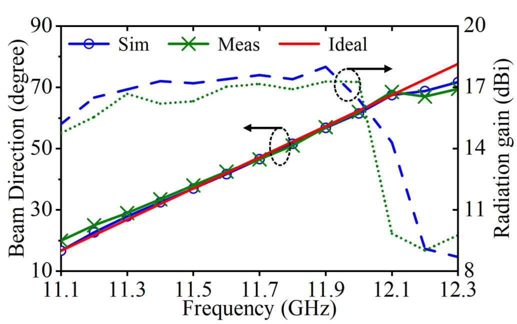

Fig. 19. Simulated and measured beam angles and radiation gains for the proposed LWA.

TABLE II
COMPARISON OF DIFFERENT HIGH RASR ANTENNAS

Reported Works	Center Frequency (GHz)	Scanning Range (deg)	RASR (deg)	Gain (dBi)
[20]	13.7	35	1198.8	>9.2
[21]	9.6	152	660.9	>9
[22]	2.5	27	337.5	<8
[23]	11.1	123	1365.3	7.3∼9.6
This Work	11.5	40.8	589.3	15.2∼18

which is especially helpful to control the scanning rate as desired. The LWA is a waveguide-type antenna operating in the TE_{30} mode, and the pins at the radiation aperture are carefully tuned to control the leakage rate. The proposed LWA can scan linearly within 50.8° from 11.1∼12.1 GHz, with good performance of radiation gain and the sidelobe level. This is applicable for relaxing the bandwidth requirement of RF transceivers and A/D converters in LWA based systems, reducing the complexity of the whole system in the meanwhile.

REFERENCES

[1] A. A. Oliner, “Leakage from higher modes on microstrip line with application to antenna,” *Radio Sci.*, vol. 22, no. 6, pp. 907–912, Nov 1987.

[2] W. Hansen, “Radiating electromagnetic waveguide,” U.S. Patent 402 622, Jun 25, 1946.

[3] J. H. Liu, D. R. Jackson, and Y. L. Long, “Substrate integrated waveguide (SIW) leaky-wave antenna with transverse slots,” *IEEE Trans. Antennas Propag.*, vol. 60, no. 1, pp. 20–29, Jan 2012.

[4] G. Zhang, Q. Zhang, Y. Chen, T. Guo, C. Caloz, and R. D. Murch, “Dispersive feeding network for arbitrary frequency beam scanning in array antennas,” *IEEE Trans. Antennas Propag.*, vol. 65, no. 6, pp. 3033–3040, June 2017.

[5] S. Gupta, S. Abielmona, and C. Caloz, “Microwave analog real-time spectrum analyzer (RTSA) based on the spectral-spatial decomposition property of leaky-wave structures,” *IEEE Trans. Microw. Theory Tech.*, vol. 57, pp. 2989–2999, Dec 2009.

[6] F. Kozak, V. Jenik, J. Machac, and P. Hudec, “Microwave radar sensor based on crlh siw Leaky-Wave antennas,” in *European Radar Conference*, 2014, pp. 53–56.

[7] S. Gruszczynski, A. Rydosz, J. Sorock, I. Slomian, P. Kaminski, and K. Wincza, “Leaky-wave antenna in multilayer structure for sensor applications,” in *International Symposium on Antennas and Propagation*, 2016.

[8] S. I. Matsuzawa, K. Sato, Y. Inoe, and T. Nomura, “Steerable composite right/left-handed leaky wave antenna for automotive radar applications,” in *Microwave Conference, 2006*, European, 2006, pp. 1155–1158.

[9] M. M. Moeini, H. Oraizi, and A. Amini, “Collimating cylindrical surface leaky waves for highly improved radiation characteristics of holograms,” *Phys. Rev. Applied.*, vol. 11, no. 4, Apr 2019.

[10] C. Vazquez, C. Garcia, Y. Alvarez, S. Ver-Hoeye, and F. Las-Heras, “Near field characterization of an imaging system based on a frequency scanning antenna array,” *IEEE Trans. Antennas Propag.*, vol. 61, no. 5, pp. 2874–2879, May 2013.

[11] O. Yurduseven, J. N. Gollub, D. L. Marks, , and D. R. Smith, “Frequency diverse microwave imaging using planar mills-cross cavity apertures,” *Opt. Exp.*, vol. 24, no. 8, pp. 8907–8925, Apr 2016.

[12] G. S. Kong, H. F. Ma, B. G. Cai, and T. J. Cui, “Continuous leaky-wave scanning using periodically modulated spoof plasmonic waveguide,” *Sci. Rep.*, vol. 6, no. 29600, pp. 1–8, Jul 2016.

[13] P. Burghignoli, G. Lovat, and D. R. Jackson, “Analysis and optimization of leaky-wave radiation at broadside from a class of 1-D periodic structures,” *IEEE Trans. Antennas Propag.*, vol. 54, no. 9, pp. 2593–2604, Sep 2006.

[14] A. Mallahzadeh and S. Mohammad-Ali-Nezhad, “Periodic collinearslotted leaky wave antenna with open stopband elimination,” *IEEE Trans. Antennas Propag.*, vol. 63, no. 12, pp. 5512–5521, Dec 2018.

[15] R. Shaw and M. K. Mandal, “Broadside scanning asymmetric siw lwa with consistent gain and reduced sidelobe,” *IEEE Trans. Antennas Propag.*, vol. 67, no. 2, pp. 823–833, Feb 2019.

[16] S. Paulotto, P. Baccarelli, F. Frezza, and D. R. Jackson, “A novel technique for open-stopband suppression in 1-d periodic printed leaky wave antennas,” *IEEE Trans. Antennas Propag.*, vol. 57, no. 7, pp. 1894–1906, Jul 2009.

[17] A. Lai, T. Itoh, and C. Caloz, “Composite right/left-handed transmission line metamaterials,” *IEEE Microw. Mag.*, vol. 5, no. 3, pp. 34–50, Sep 2004.

[18] L. Wang, J. L. Gómez-Tornero, E. Rajo-Iglesias, and O. Quevedo-Teruel, “Low-dispersive leaky-wave antenna integrated in groove gap waveguide technology,” *IEEE Trans. Antennas Propag.*, vol. 66, no. 11, pp. 5727–5736, Nov 2018.

[19] J. Chen, W. Yuan, C. Zhang, W. X. Tang, L. Wang, Q. Cheng, and T. J. Cui, "Wideband leaky-wave antennas loaded with gradient metasurface for fixed-beam radiations with customized tilting angles," *IEEE Trans. Antennas Propag.*, vol. 68, no. 1, pp. 161–170, Jan 2020.

[20] D. F. Guan, Q. Zhang, P. You, Z. B. Yang, Y. Zhou, and S. W. Yong, "Scanning rate enhancement of leaky wave antennas using slow-wave substrate integrated waveguide (siw) structure," *IEEE Trans. Antennas Propag.*, vol. 66, no. 7, pp. 3747–3751, Jul 2018.

[21] G. Zhang, Q. Zhang, Y. Chen, and R. D. Murch, "High-scanning-rate and wide-angle leaky-wave antennas based on glide-symmetry goubau line," *IEEE Trans. Antennas Propag.*, vol. 68, no. 4, pp. 2531–2540, Apr 2020.

[22] G. Zhang, Q. Zhang, S. Ge, Y. Chen, and R. D. Murc, "High scanning-rate leaky-wave antenna using complementary microstrip-slot stubs," *IEEE Trans. Antennas Propag.*, vol. 67, no. 5, pp. 2913–2922, May 2019.

[23] S. Xu, D. Guan, Q. Zhang, P. You, S. Ge, X. Hou, Z. Yang, and S. Yong, "A wide-angle narrow-band leaky-wave antenna based on substrate integrated waveguide-spoof surface plasmon polariton structure," *IEEE Antenn. Wirel. PR.*, vol. 18, no. 7, pp. 1386–1389, Jul 2019.

[24] D. R. Jackson, C. Caloz, and T. Itoh, "Leaky-wave antennas," *Proc. IEEE.*, vol. 100, no. 7, pp. 2194–2206, Jul 2012.

[25] S. Amari, R. Vahldieck, and J. Bornemann, "Accurate analysis of periodic structures with an additional symmetry in the unit cell from classical matrix eigenvalues," *IEEE Trans. Microw. Theory Techn.*, vol. 46, no. 10, pp. 1513–1515, Oct 1998.

[26] G. Valerio, Z. Sipus, A. Grbic, and O. Quevedo-Teruel, "Accurate equivalent-circuit descriptions of thin glide-symmetric corrugated metasurfaces," *IEEE Trans. Antennas Propag.*, vol. 65, no. 5, pp. 2695–2700, May 2017.

[27] M. Camacho, R. C. Mitchell-Thomas, A. P. Hibbins, J. R. Sambles, and O. Quevedo-Teruel, "Mimicking glide symmetry dispersion with coupled slot metasurfaces," *Appl. Phys. Lett.*, vol. 111, no. 12, 2017.

[28] F. Mesa, R. Rodríguez-Berral, and F. Medina, "On the computation of the dispersion diagram of symmetric one-dimensionally periodic structures," *Symmetry*, vol. 10, no. 8, 2018.

[29] M. Bagheriasl and G. Valerio, "Bloch analysis of electromagnetic waves in twist-symmetric lines," *Symmetry*, vol. 11, no. 5, 2019.

[30] Z. Sipus and M. Bosiljevac, "Modelling of glide-symmetric dielectric structures," *Symmetry*, vol. 11, no. 6, 2019.

[31] N. Memeletzoglou, C. Sanchez-Cabello, F. Pizarro-Torres, and E. Rajo-Iglesias, "Analysis of periodic structures made of pins inside a parallel plate waveguide," *Symmetry*, vol. 11, no. 4, 2019.

[32] M. Ebrahimpouri, A. A. Brazalez, L. Manholm, and O. Quevedo-Teruel, "Using glide-symmetric holes to reduce leakage between waveguide flanges," *IEEE Microw. Compon. Lett.*, vol. 28, no. 6, pp. 473–475, June 2018.

[33] A. Vosoogh, H. Zirath, and Z. S. He, "Novel air-filled waveguide transmission line based on multilayer thin metal plates," *IEEE Trans. THz Sci. Technol.*, vol. 9, no. 3, pp. 282–290, May 2019.

[34] E. Rajo-Iglesias, M. Ebrahimpouri, , and O. Quevedo-Teruel, "Wideband phase shifter in groove gap waveguide technology implemented with glide-symmetric holey ebg," *IEEE Microw. Compon. Lett.*, vol. 28, no. 6, pp. 476–478, Jun 2018.

[35] A. Palomares-Caballero, A. Alex-Amor, P. Padilla, F. Luna, and J. Valenzuela-Valdes, "Compact and low-loss v-band waveguide phase shifter based on glide-symmetric pin configuration," *IEEE Access*, vol. 7, pp. 31 297–31 304, Mar 2019.

[36] A. Monje-Real, N. J. G. Fonseca, O. Zetterstrom, E. Pucci, and O. Quevedo-Teruel, "Holey glide-symmetric filters for 5G at millimeter-wave frequencies," *IEEE Microw. Compon. Lett.*, vol. 30, no. 1, pp. 31–34, Jan 2020.

[37] O. Quevedo-Teruel, M. M. J. Miao, A. Algaba-Brazalez, M. Johansson, and L. Manholm, "Glide-symmetric fully metallic luneburg lens for 5G communications at Ka-band," *IEEE Antenn. Wirel. PR.*, vol. 17, no. 9, pp. 1588–1592, Sep 2018.

[38] M. Vukomanovic, J. L. Vazquez-Roy, O. Quevedo-Teruel, E. Rajo-Iglesias, and Z. Sipus, "Gap waveguide leaky-wave antenna," *IEEE Trans. Antennas Propag.*, vol. 64, no. 5, pp. 2055–2060, Mar 2016.

[39] M. Memarian and G. V. Eleftheriades, "Dirac leaky-wave antennas for continuous beam scanning from photonic crystals," *Nat. Commun.*, vol. 5855, no. 5855, Jan 2015.

[40] O. Dahlberg, R. C. Mitchell-Thomas, and O. Quevedo-Teruel, "Reducing the dispersion of periodic structures with twist and polar glide symmetries," *Sci Rep.*, vol. 7, no. 1, 2017.

[41] D. M. Pozar, *Microwave engineering*, 4th ed. NJ: Wiley, 2012.

[42] H. Wang, R. Gao, Y. Gu, J. Cao, and Z. Ye, "Low sidelobe leaky wave antenna based on gap waveguide technology," in *Applied Computational Electromagnetics Society Symposium (ACES)*, Aug 2017, pp. 1–2.

[43] L. Wang, Q. Cheng, W. Tang, X. Yin, and O. Quevedo-Teruel, "On the enhancement of scanning and gain flatness of leaky-wave gap-waveguide antennas with glide symmetry," in *2019 13th Europ. Conf. Antennas Propag. (EuCAP)*, Krakow, Poland, 2019, pp. 1–4.

[44] J. Chen, Q. Cheng, W. Yuan, W. X. Tang, L. Wang, and T. J. Cui, "Generation of high-order waveguide modes with reduced symmetric protection," *Phys. Rev. Applied.*, vol. 024040, no. 14, Aug 2020.

Jianfeng Chen received the B.S. degree in physics from Nanjing Normal University, Nanjing, China, in 2009, and the M.S. degree in electromagnetic field and microwave technology from Nanjing University of Science and Technology, in 2014. He is currently working toward the Ph.D degree at the State Key Laboratory of Millimeter Waves, Department of Radio Engineering, Southeast University, Nanjing. His current research interests include metamaterials with higher symmetry, leaky-wave antennas and microstrip patch antennas.

Wei Yuan was born in Jiangsu, China. He received the B.S. degree in electrical & information engineering from Xidian University, Xi'an, China, in 2015. He is currently working toward the Ph.D degree at the State Key Laboratory of Millimeter Waves, Department of Radio Engineering, Southeast University, Nanjing.

His current research interests are lens antennas, metamaterials with higher symmetry and Fabry-Perot resonator antennas.

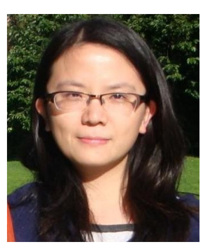

Wen Xuan Tang (S'10–M'13)received the B.Sc. degree and the M.Sc. degree from Southeast University, Nanjing, China, in 2006 and 2009, respectively, and the Ph.D. degree in electromagnetics from the Queen Mary University of London, London, U.K., in 2012. In 2012, she joined the School of Information Science and Engineering, Southeast University, Nanjing, China. She is currently an Associate Professor in State Key Laboratory of Millimeter Waves at Southeast University. She has authored / co-authored over 40 journal articles, one book and two book chapters on metamaterials and their applications, and has been invited to give presentations at several international conferences. She is currently an associate editor of Advanced Electromagnetics (AEM), and a guest editor of the journal of EPJ Applied Metamaterials (EPJ AM). Her current research interests include metamaterials and their applications, and microwave devices and antennas.

This article has been accepted for publication in a future issue of this journal, but has not been fully edited. Content may change prior to final publication. Citation information: DOI 10.1109/TAP.2020.3037830, IEEE Transactions on Antennas and Propagation

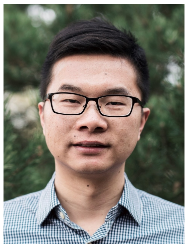

Lei Wang (S'09-M'16-SM'19) received the Ph.D. degree in electromagnetic field and microwave technology from the Southeast University, Nanjing, China in 2015. From September 2014 to September 2016, he was a Research Fellow and Postdoc in the Laboratory of Electromagnetics and Antennas, Swiss Federal Institute of Technology (EPFL) in Lausanne, Switzerland. From October 2016 to November 2017, he was a Postdoc Research Fellow in Electromagnetic Engineering Laboratory of KTH Royal Institute of Technology in Stockholm, Sweden. From November 2017 to February 2020, he was an Alexander von Humboldt scholar in the Institute of Electromagnetic Theory of Hamburg University of Technology (TUHH) in Hamburg, Germany. From March 2020 to present, he is an Assistant Professor in the Institute of Signals, Sensors and Systems of Heriot-Watt University in Edinburgh, United Kingdom. His research includes the antenna theory and applications, active electronically scanning arrays, integrated antennas and arrays, substrate-integrated waveguide antennas, leaky-wave antennas, and wireless propagations.

He was awarded the Chinese National Scholarship for PhD Candidates in 2014 and was granted the Swiss Government Excellence Scholarship to conduct research on SIW horn antennas and applications in 2014 too. He was also granted by the Alexander von Humboldt Research Foundation to take research on antenna modelling and optimization in 2016. Moreover, he received the Best Poster Award in 2018 IEEE International Workshop on Antenna Technology (iWAT) and the Best Paper Award in the 5th International Conference on the UK-China Emerging Technologies (UCET2020).

Qiang Cheng (M'15) received the B.S. and M.S. degrees from the Nanjing University of Aeronautics and Astronautics, Nanjing, Jiangsu, China, in 2001 and 2004, respectively, and the Ph.D. degree from Southeast University, Nanjing, in 2008.

In 2008, he joined the State Key Laboratory of Millimeter Waves, Southeast University, where he was involved in the development of metamaterials and metadevices. He is currently a Full Professor with the Radio Department, Southeast University. He leads a group of Ph.D. students and master students in the area of metamaterials, tunable microwaves circuits, microwave imaging, and terahertz systems. He has authored or co-authored more than one hundred publications, with citation over 2000 times.

Dr. Cheng was a recipient of the 2010 Best Paper Award from the New Journal of Physics, the China's Top Ten Scientific Advances of 2010, and the Second Class National Natural Science Award in 2014. He served as the Vice Chair for the 2008 and 2010 International Workshop on Metamaterials, Nanjing, China.

Tie Jun Cui (M'98-SM'00-F'15) received the B.Sc., M.Sc., and Ph.D. degrees in electrical engineering from Xidian University, Xi'an, China, in 1987, 1990, and 1993, respectively. In 1993, he joined the Department of Electromagnetic Engineering, Xidian University, and was promoted to an Associate Professor in 1993. From 1995 to 1997, he was a Research Fellow with the Institut fur Hochstfrequenztechnik und Elektronik, University of Karlsruhe, Germany. In 1997, he joined the Center for Computational Electromagnetics, Department of Electrical and Computer Engineering, University of Illinois at Urbana–Champaign, Champaign, IL, USA, first as a Postdoctoral Research Associate and then a Research Scientist. In 2001, he became a Cheung-Kong Professor with the Department of Radio Engineering, Southeast University, Nanjing, China. He is now the Chief Professor of Southeast University. He is the first author of books *Metamaterials-Theory, Design*, and *Applications* (Springer, Nov. 2009) and *Metamaterials: Beyond Crystals, Noncrystals, and Quasicrystals* (CRC Press, Mar. 2016). He has authored or coauthored over 400 peer-reviewed journal papers, which have been cited by more than 23000 times (H-factor 76).

Dr. Cui received many honors and awards, including the Research Fellowship from the Alexander von Humboldt Foundation, Bonn, Germany (1995), Young Scientist Award from the International Union of Radio Science (1999), Cheung Kong Professor under the Cheung Kong Scholar Program (2001), National Science Foundation of China for Distinguished Young Scholar (2002), Special Government Allowance awarded by the Department of State, China (2008), Award of Science and Technology Progress from Shaanxi Province Government (2009), the May 1st Labour Medal from Jiangsu Province Government (2010), Award of Natural Science (First Class) from the Ministry of Education, China (2011), Awards of National Natural Science of China (Second Class, 2014 and 2018). His research has been selected as one of the "Optics in 2016" by Optics and Photonics News Magazine (OSA), 10 Breakthroughs of China Science in 2010, "Best of 2010" in New Journal of Physics, and Research Highlights in Europhysics News, Journal of Physics D: Applied Physics, Applied Physics Letters, and Nature China. His work has been reported by Nature News, Science, MIT Technology Review, Scientific American, and New Scientists. He was an Associate Editor of IEEE Transactions on Geoscience and Remote Sensing, Guest Editors of Research, Science Bulletin, and Science China, and Editorial Staff for IEEE Antennas and Propagation Magazine. He served as General Co-Chair for International Workshops on Metamaterial in 2008 and 2012, TPC Co-Chair for Asian Pacific Microwave Conference in 2005, TPC Co-Chair for Progress in Electromagnetic Research Symposium in 2004. According to ELSEVIER, he is one of the most cited Chinese researchers.